Int. J. Heat Mass Transfer. Vol. 7, pp. 1223–1234. Pergamon Press 1964. Printed in Great Britain

THE EFFECT OF DIAMETER SIZE AND SPEED OF ROTATION ON THE HEAT TRANSFER FROM STEAM TO COOLED CYLINDERS

RUSSELL HOYLE* and D. H. MATTHEWS†

(*Received* 21 *December* 1963)

Abstract—An apparatus for measuring the transfer of heat from a steam atmosphere to cooled rotating cylinders on which the steam was condensing is described. Three cylinders were used of 4, 8, and 10 in dia. each being cooled internally by water. The magnitude of the heat flux from the steam atmosphere was calculated from measurements taken of the temperature gradients through the rotor walls. A comparison was made in the stationary case between the measured results and those calculated from Nusselt's equation. For the rotational case Nusselt's equation has been modified, and it has been shown how this modified equation can be used in calculating heat-transfer coefficients for any temperature, diameter, and speed of rotation within the ranges considered. The ranges of speed were from 0 to 1500 rev/min, and of steam condensation temperature from 220°F to 310°F, and of temperature difference between steam and rotor between 6 and 50 degF. These ranges cover conditions existing in many steam turbines while starting from cold, and in some rotary condensers.

NOMENCLATURE

c, specific heat of condensate [Btu/lb degF];
g, gravitational constant [ft/s^2];
h, heat-transfer coefficient [Btu/ft^2 h degF];
k, thermal conductivity of condensate [Btu/ft h degF];
$\dot{q}''$, heat flux [Btu/ft^2 h];
w, speed of rotation [rad/h];
D, D_1, external and internal diameters [ft];
H, height [ft];
l, enthalpy of evaporation [Btu/lb];
M_1, total mass flow rate per unit length [lb/h ft];
Pr, Prandtl number, $c\mu/k$;
Re, Reynolds number, $D^2w\rho/2\mu$, for rotating cylinders;
T_f, mean temperature of condensate [°F];
T_0, T_1, temperatures of external and internal surface of shaft [°F];
T_s, condensation temperature of steam [°F];
μ, dynamic viscosity of condensate [lb/ft h];
ρ, density of condensate [lb/ft^3];
σ, surface tension of condensate [lb/ft];
θ, temperature difference [degF];
θ_s, $(T_s - T_0)$ [degF];
θ_w, $(T_0 - T_1)$ [degF];
ϕ, an angle [rad];

* Imperial College, London, S.W.7.
† 86, Fields Park Road, Newport, Monmouthshire.

1. INTRODUCTION

Nusselt's basic theory of filmwise condensation heat transfer

NUSSELT [1] in 1916 produced an important and most generally accepted theory for determining heat-transfer rates for condensing vapours. He considered five fundamental cases of condensation.

(i) vapours condensing on a smooth plane surface making an angle ϕ with the horizontal, assuming that the vapour was pure and saturated and relatively stationary with respect to the condensate;
(ii) vapour condensing on the outside of a horizontal tube under the above conditions;
(iii) vapour condensing on a surface as in (i) but with appreciable vapour velocity;
(iv) superheated vapour condensing on any surface;

(v) vapour condensing on any surface with the vapour impure.

In order to simplify the mathematics of the problem Nusselt made the following assumptions:

(i) The film of condensate is thin and in laminar flow on a clean isothermal surface;
(ii) The temperature gradient through the condensate can be taken as a straight line, and the physical properties of the condensate can be assumed to be at a mean film temperature;
(iii) The curvature of the condensate film can be neglected;
(iv) For condensation of superheated vapour the vapour is first cooled, as if it were a gas, to the saturation temperature and can then be treated by the method for saturated vapour.

The equations derived by Nusselt are as follows,

For vertical surfaces:

$$h_m = 0{\cdot}94\ (l\ \rho^2\ k^3\ g/\mu\ H\ \theta)^{1/4}$$

For inclined flat surfaces:

$$h_m = 0{\cdot}94\ (l\ \rho^2\ k^3\ g/\mu\ H\ \theta \sin\phi)^{1/4}$$

For horizontal tubes:

$$h_m = 0{\cdot}72\ (l\ \rho^2\ k^3\ g/\mu\ D\ \theta)^{1/4}$$

where h_m is the mean heat-transfer coefficient, and in the case of the surfaces H the height of one end of a surface above the other, and ϕ is the angle between the horizontal and the surface.

Generally in experimental cases, when Nusselt's assumptions are made, the results give good agreement with theory, although the measured heat-transfer rates are a little above those given by the theory.

Measurements of heat transfer from steam to a rotating cylinder were described by Yeh [2]. The cylinder used by him was of 1 in dia. only. The purpose of the research reported here was, primarily, to study the effect in similar circumstances of changes of diameter as well as speed of rotation. It was the author's intention to measure the heat transfer from steam to cooled rotating cylinders of various sizes and to attempt to develop a formula that would enable heat-transfer coefficients to be found for a range of size of diameters and of speeds.

2. APPARATUS

Essentially the apparatus with which the heat-transfer measurements were made consisted of a casing enclosing a steam atmosphere in which a cooled cylinder was made to rotate.

2.1 *The casing*

A general view of the 8 in dia. rotor in position in the casing is shown at 1, 2, and 3 in Fig. 1. The casing was designed for a working pressure of 200 lb/in² gauge, and had an internal diameter of 16 in, a length of 13 in, and was made in two halves with horizontal flanges.

To seal the steam, segmented carbon rings were provided to act as labyrinth seals at 4 in Fig. 1, and the shaft was chromium plated at this part to prevent corrosion.

Before entering the casing the steam was passed through two large water separators, and

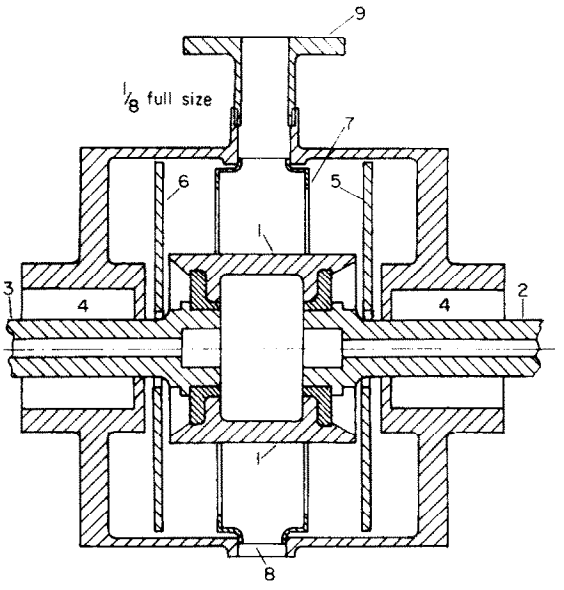

1. Rotor
2. Shaft
3. Shaft
4. Gland
5. Perforated plate
6. Perforated plate
7. Condensate collector
8. Condensate drain
9. Access pipes

FIG. 1. General view of a rotor in position in the casing.

then to an orifice-plate flowmeter and manometer, and finally to a throttling calorimeter. The steam, having entered the bottom half of the casing, passed through the perforated steel plate 5 to the working section of the casing, over the surface of the rotor on which some of it was condensed, and out through another perforated steel plate 6 to the outlet manifold.

To enable the condensate to be collected a sheet-steel condensate collector 7 was fitted inside the vessel. Condensate that had been thrown off, or drained from the rotor's lowest point by gravity, struck the collector and was taken from the casing at 8 to a steam trap.

Five 2-in pipes and flanges, 9 in Fig. 1, were provided to give access to the interior of both the casing and the condensate collector. These were used to illuminate the rotor by an electric flash illumination tube and to photograph it.

2.2 *The rotor*

The 8 in dia. rotor is shown in position in Fig. 1, and in more detail in Fig. 2, and two other similar rotors were used of 10 and 4 in outside dia.

The cylindrical surfaces of the rotors were made of mild steel and were plated, internally and externally, with a 0·001 in thick layer of nickel to prevent corrosion and ensure that a stable state of surface was maintained throughout the tests. The thermal conductivity was measured by the non-destructive thermal comparator method devised by Powell [8].

After passing through separators, to avoid air being carried into the rotor, cooling water was supplied at point 1 in Fig. 2 and passed over the deflector, item 2, in the directions shown in Fig. 2 by arrows. If, in spite of precautions, air entered the rotor it could be concentrated at the centre by centripetal force and then expelled by applying a high flow rate of cooling water.

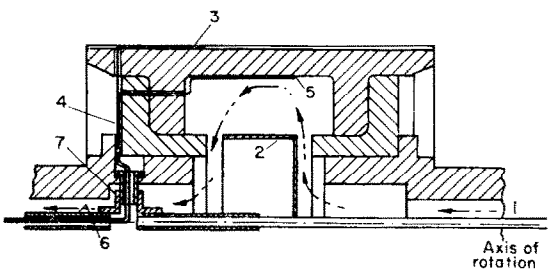

FIG. 2. Section of half the 8 in rotor.

Twelve slots, item 3 in Fig. 2, to hold the copper-constantin thermocouple leads were milled on the rotors' external surfaces and radially on the end plates, 4. On the internal surface the thermocouple junctions, 5, were attached by a thin layer of soft solder. All the thermocouple leads for a length from the bead of at least ten diameters were laid along an estimated isothermal.

The positions of the thermocouples in the 10 in rotor are shown in Fig. 3 in terms of axial

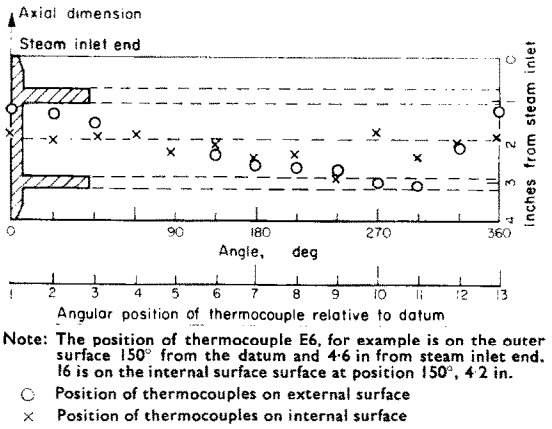

Note: The position of thermocouple E6, for example is on the outer surface 150° from the datum and 4·6 in from steam inlet end. I6 is on the internal surface surface at position 150°, 4·2 in.

○ Position of thermocouples on external surface

× Position of thermocouples on internal surface

FIG. 3. Position of thermocouples on the 10 in rotor.

length and circumferential angle. Thermocouples were also fixed to the end plate on the flange-studs pitch circle, and, to measure the cooling-water temperatures, four pairs of thermocouple leads were taken into the water space.

Electrical connection was made between the thermocouples on the rotating shaft and stationary instruments by means of mercury slip rings. These consisted of a series of rotating copper disks separated by Perspex rings and mounted on a Tufnol shaft with their rims dipping in stationary pools of mercury.

2.3 *Preparation*

The rotor's external nickel-plated surface was cleaned of grease and, when in position in the casing, was washed with carbon tetrachloride and then alcohol to dissolve grease. The surface was polished lightly with fine emery, rubbed with

fine abrasive powder on a moistened cloth, and finally washed with water. This process was repeated until the surface was completely wettable by water.

Before testing, after steam had been raised, steam traps and drain cocks were opened to enable the initial flow of condensate to drain freely and to blow out all air. The traps were then set to pass any separated water and the apparatus was left with the steam on for 30 min. The range of steam pressure used in the tests was from 20 to 80 lb/in^2 abs.

3. THE TEST RESULTS

3.1 *Experimental values of heat-transfer coefficients*

The experimental values of heat flux $\dot{q}''$, for both the stationary and rotational cases, were found from the following equation for heat flow through a thick-walled cylinder in which

$$\dot{q}'' = 2\,k_w\,\theta_w/D\,\log_e\,(D/D_1) \qquad (1)$$

where k_w is the thermal conductivity of the material and θ_w is the difference $T_0 - T_1$ between the temperatures at the outer and inner diameters D and D_1 respectively.

The experimental heat-transfer coefficient was found from the following equation,

$$h_e = \dot{q}''/\theta_s = 2\,k_w\,\theta_w/D\,\theta_s\,\log_e\,(D/D_1) \qquad (2)$$

and experimental values of $\dot{q}''$ and h_e discussed later in this paper have all been found by using experimentally derived values of θ_w and θ_s in equations (1) and (2).

3.2 *Stationary test results*

In the stationary tests, sets of readings were taken for each of six positions of the rotor 60° apart. Figure 4 shows a set of results from one typical stationary test on the 10 in dia. rotor, and similar curves are available for other tests on this rotor and for tests on the 8 and 4 in rotors. Smooth curves have been drawn in Fig. 4 showing the distribution of temperature around the periphery of the cylinder. Individual thermocouple reference numbers are shown against each curve and the key to these is given in Fig. 3.

A feature that is common to all test results is the dip in the readings around 270° angle which is the bottom of the rotor. The condensate flows down the sides of the rotor and thickens the layer of condensate at the bottom before it breaks away and falls to the bottom of the casing. The rate of heat flow through the thickened layer at the bottom of the rotor is less than that through the condensate on the sides and top of the rotor, and consequently the temperature of the rotor wall was reduced at this position.

3.2.1 *Correction of stationary results.* In the ideal case the temperature distribution would be uniform along the axis, but the relative positions of the curves in Fig. 4 show that the

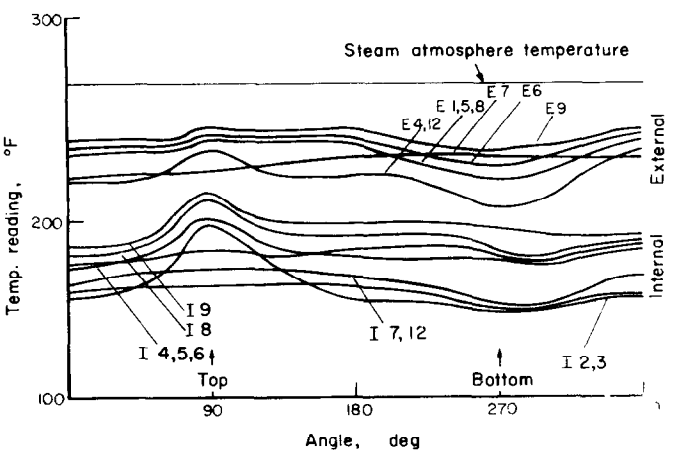

FIG. 4. Variation of temperature with angular position in stationary test.

experimental axial temperature distributions were not uniform, due primarily to heat losses at the ends. These are influenced by

(*a*) the nature of the junction between the ends of the cylinders and the end plates,
(*b*) the amount of entrapped air from the cooling water, which will increase the end losses by cutting down radial flow.

The curves in Fig. 4 display high temperatures, especially at the internal surface, at the top of the rotor—that is at 90° angle from the datum—due to air coming out of solution from the cooling water and being trapped at the highest point inside the rotor. In rotational tests the air was easily got rid of in the manner already described, and therefore rotational results were not affected. In the stationary tests the readings that were affected were corrected by replacing all the readings in the 90° region by others not in but near the 90° region.

Small apparent deviations from axial uniformity were caused also by thermocouple junctions being not quite on the external and internal surfaces and their depths below the surface, although of unknown magnitude, were expected to vary. The deviations from this cause were expected to be small.

It is on the 10 in rotor that the axial temperature distributions were most nearly uniform, and the heat flow was most nearly radial, and therefore the results on the 10 in rotor agree most nearly with Nusselt's values. In the cases reported here the mean disagreements between the experimental values from equation (2) and the theoretical values from Nusselt's equation (3), had values of −1080, +6800, and +7400 Btu/ft² h, which are approximately −4, 21, and 15 per cent of the arithmetic mean of all the heat fluxes for each rotor.

It is believed that these mean disagreements between experimental and theoretical stationary values represent fairly a disagreement between experimental and theoretical values as defined above for the range of tests including the rotational tests. Therefore the corrections given above have been added to all experimental figures for heat flux, and are intended to correct for end losses and for thermocouples not being precisely on the surface.

3.2.2 *Comparison of experimental with theoretical stationary values.* In the preceding paragraph the stationary experimental results have been compared with Nusselt's theoretical values. This is justified in stationary cases if the flow of the condensate is laminar, which it was expected to be because turbulence appears when Reynolds number exceeds the critical value of 2100 [3]. Reynolds number can be found from the expression,

$$Re = 2\,M_1/\mu$$

where M_1 is the total mass flow rate per unit length. M_1 in this case was found by dividing the heat flux $\dot{q}''$ by the product of the latent heat and the periphery of the shaft, giving values for M_1 of 73·2 and 104·6, and hence for Re of 209 and 298, for the 4 and 10 in rotors respectively, considerably lower than the critical value of 2100.

In Table 1 stationary experimental values of the heat-transfer coefficients measured on all rotors and corrected as described above are shown, and compared with Nusselt values calculated from equation (3), and also with the coefficients calculated by use of the equation (10) which is the equation recommended for use in the rotational case.

3.3 *Rotational tests*

For the rotational tests about 65 tests were performed on each of the three rotors. The procedure employed was to run the rotor at constant speed and vary the steam pressure and cooling-water conditions to achieve the desired heat flow at that speed. For each rotor from 6 to 9 different speeds were used, ranging from stationary to 1500 rev/min.

Figure 5 shows a set of results from one typical rotational test on the 10 in dia. rotor at 597 rev/min plotted against time.

Having obtained results such as those shown in Fig. 5 the experimental values of $\dot{q}''$ were calculated by inserting in equation (1) values of θ_w taken from the five sets of readings of the middle thermocouples E5 and I5, so obtaining five values of $\dot{q}''$ giving one mean value to which the correction figure was added. From the mean values for $\dot{q}''$, and mean values for θ_s, experimental values of the heat-transfer coefficients,

Table 1. Stationary values of heat-transfer coefficient

Diameter (in)	Test No.	θ_s (degF)	T_s (°F)	T_f (°F)	h^* Nusselt equation (3)	h^* Measured equation (2)	h^* From rotational equation (10)
4	14	26	230	211	1460	1350	1460
	15	32	249	225	1380	1460	1400
	16	39	259	229	1320	1380	1330
	17	49	287	250	1280	1230	1280
	18	21	234	218	1540	1490	1520
8	15	23	261	243	1300	1330	1160
	22	32	256	232	1190	1160	1050
	66	40	258	228	1160	870	990
	67	50	293	254	1080	780	970
10	18	26	236	215	1150	1160	960
	19	29	236	215	1130	1110	960
	20	33	260	236	1110	1080	940
	21	42	293	260	1060	1010	880
	22	43	305	272	1050	1060	880
	23	22	235	217	1230	1300	1010

* None of the heat-transfer coefficients quoted here are local coefficients; like Nusselt's values they are mean coefficients for the whole circumference of the cylinder.

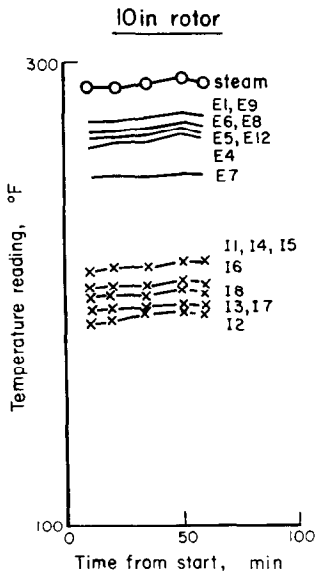

FIG. 5. Results of a rotational test at 597 rev/min.

h_e, were obtained using equation (2). These are the values shown plotted against $\theta_s(1/c\ \theta_s)^{1/4}$ in Fig. 7(a) and (b) for the 10 in rotor.

4. DEVELOPMENT OF A RECOMMENDED FORMULA

4.1 *The independent variables*

For steam condensing on a rotating shaft the heat flux $\dot{q}''$ and the heat-transfer coefficient h are dependent on the following independent variables,

(i) T_s the steam condensation temperature;
(ii) θ_s the difference between T_s and T_0 the temperature of the outer surface of the rotor;
(iii) w the speed of rotation;
(iv) D the rotor diameter;
(v) the nature of the surface of the rotor.

The dependence of heat flux on these must be the basis of any recommended formula.

Consideration of the range of Reynolds numbers mentioned in section 3.2.2 for the stationary case, and of the photography [4] in the rotational case, led us to believe that throughout the tests the condensate layer was in laminar flow. The equation used to calculate theoretical values of heat flow through a stationary horizontal cylinder in the case of

laminar flow under natural gravitational force can be expressed [5] as very nearly,

$$h = 0{\cdot}733\, k\, (g\, \rho^2/D\, \mu^2)^{1/4}\, (c\, \theta_s/l\, Pr)^{-1/4} \quad (3)$$

for condensate with Prandtl number 1 to 1000 and $(c\, \theta_s/l)$ up to 0·01. In using this equation the temperature T_f at which the physical properties of the condensate were evaluated was found from the expression

$$T_f = T_s - 3\, \theta_s/4 \quad (4)$$

In developing a useful formula it was thought possible to replace the constant 0·733 by a non-dimensional variable depending on the five independent variables by including particularly their effect on condensate flow, vapour drag, disturbance due to throwing off drops, and variations in surface tension. This is similar to a method used by Sparrow and Gregg for condensation on a rotating disk [6a and 6b].

In equation (5) therefore 0·733 has been replaced by a variable B_1 as a step to obtaining an expression for h in the case of a rotor. Therefore, for rotating cylinders,

$$h = B_1\, k\, (g\, \rho^2/D\, \mu^2)^{1/4}\, (c\, \theta_s/l\, Pr)^{-1/4}$$
$$= B_1\, (k^3\, g\, \rho^2\, c/D\, \mu)^{1/4}\, (l/c\, \theta_s)^{1/4} \quad (5)$$

and

$$\dot{q}'' = B_1\, (k^3\, g\, \rho^2\, c/D\, \mu)^{1/4}\, \theta_s\, (l/c\, \theta_s)^{1/4} \quad (6)$$

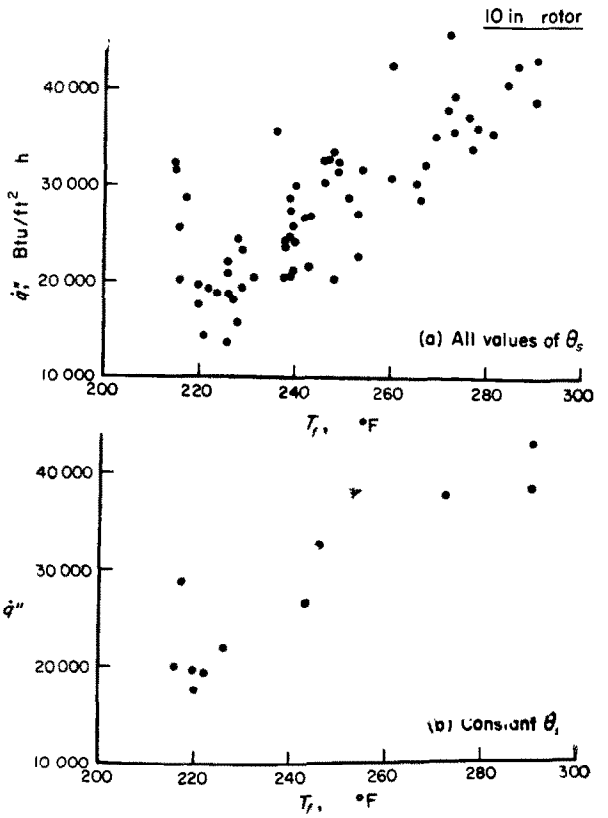

FIG. 6. Variation of heat flux with temperature.

4.2 *Variation of heat flux with steam temperature*

Considering now the first of the five independent variable listed in 4.1, equation (6) states that the heat flux is dependent on T_s in that l is dependent on T_s, and k, ρ, μ, and c are all dependent on T_f which is closely related to T_s through equation (4).

To study the variation with temperature of the experimental values of $\dot{q}''$ derived from equation (2), all values for the 10 in rotor have been plotted against steam temperature in Fig. 6(a) where an increase of $\dot{q}''$ with increase of T_f is observed. The temperature difference θ_s is independent of T_f, and in Fig. 6(b) therefore only those values of heat flux $\dot{q}''$ that are associated with values of θ_s between 20·0 and 22·3 degF are plotted against T_f. These then are experimental values of $\dot{q}''$ for nearly constant θ_s, and these confirm an increase of $\dot{q}''$ with T_s.

4.3 *Variation of heat flux with temperature difference* θ_s

Now consider θ_s, the second of the five variables listed in Section 4.1. In equation (6) it appears as a variable in the function $\theta_s\, (l/c\, \theta_s)^{1/4}$. In this, as in Sparrow and Gregg's work [6c and 6d], the dimensionless parameter $(l/c\theta_s)$ has been introduced to take account of variations in (*a*) enthalpy of evaporation l, and (*b*) the undercooling $c\theta_s$ of the condensate below saturation temperature.

All the experimental values of heat flux $\dot{q}''$, derived from measurements taken from the 10 in rotor and from equation (1), have been grouped together in nearly uniform speeds. For each group of speeds the values of $\dot{q}''$ have been plotted, in Fig. 7, against $\theta_s\, (l/c\, \theta_s)^{1/4}$. The best lines, judged by eye, have been drawn through these experimental points, and these

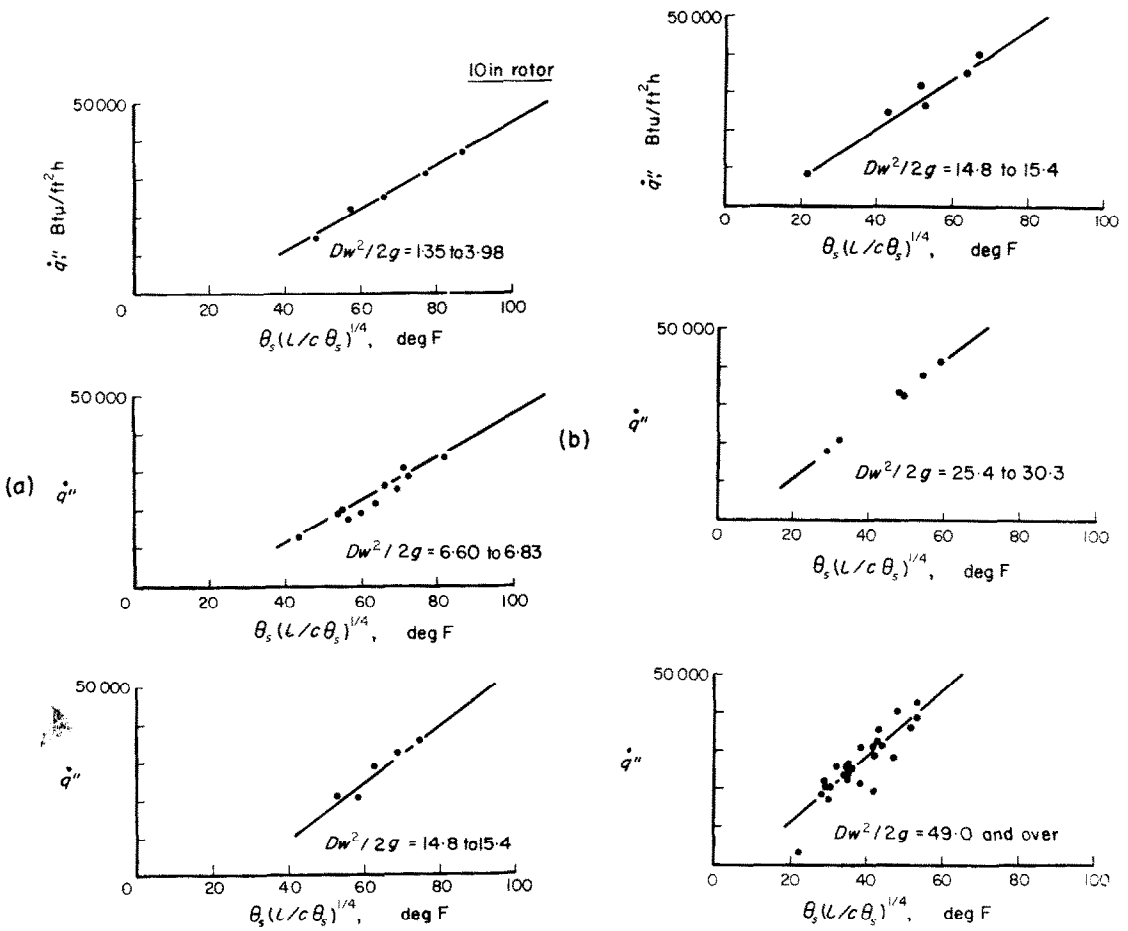

FIG. 7. Variation of heat flux with $\theta_s(l/c\,\theta_s)^{1/4}$.

have been used to derive the solid lines shown in Fig. 8 where a dimensionless heat-transfer number $(hD/2k_A)$ is shown plotted against the dimensionless number $(l/c\,\theta_s)^{1/4}$, where k_A is the thermal conductivity of water at the condensation temperature of water under normal atmospheric conditions. Similar curves for the 8 and 4 in rotors are shown by the solid lines in Figs. 9 and 10.

4.4 *Variations of heat flux with speed of rotation w and rotor diameter D*

In common with other workers [7] we attempted to correlate our results with the Weber number

$$[D\sqrt{(\rho/\sigma)}]^2\,(D\,w^2/2\,g)/2 \qquad (7)$$

but found it more easily justifiable to consider the non-dimensional terms $[D\sqrt{(\rho/\sigma)}]$ and $(D\,w^2/2g)$ separately.

The values plotted as solid lines in Fig. 8 are experimental values of $(hD/2\,k_A)$ using values of h derived from equation (2). The slopes of these solid lines are observed to vary with $(D\,w^2/2g)$, although for any one rotor and any one steam temperature all terms of equation (5) remain constant with speed except B_1. The relationship between B_1 and $(D\,w^2/2g)$ that most nearly describes these variations of slope is

$$B_1 \propto (1{\cdot}9 - 0{\cdot}9/1{\cdot}095^{D\,w^2/2g}) \qquad (8)$$

The term B_1 must also express the effect of the disruption of the film due to the throwing off of

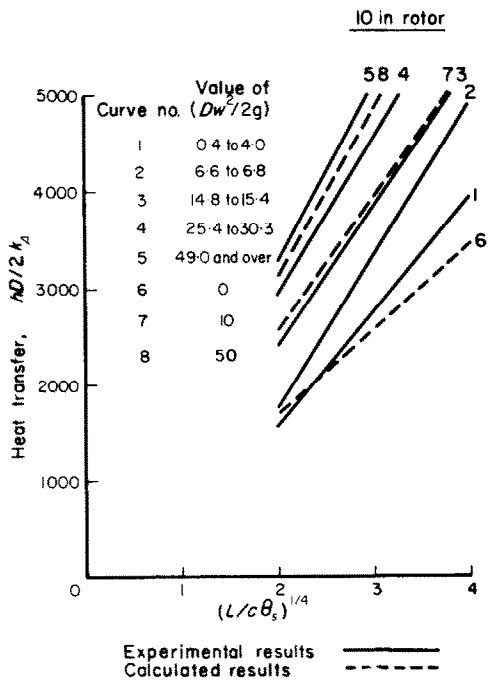

FIG. 8. Comparison of calculated with experimental results for the 10 in rotor.

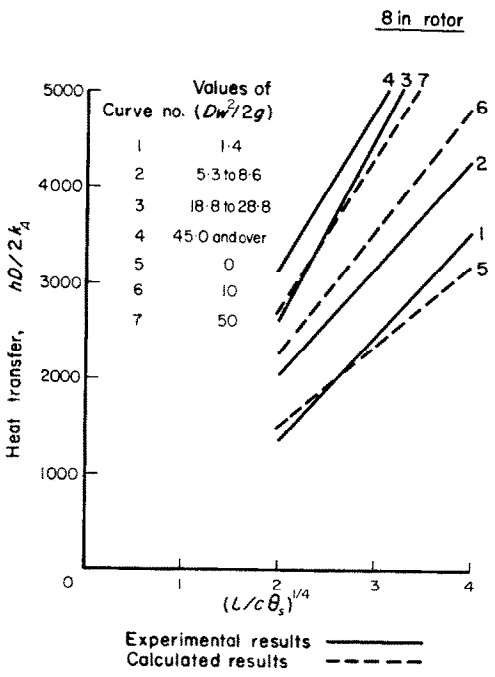

FIG. 9. Comparison of calculated with experimental results for the 8 in rotor.

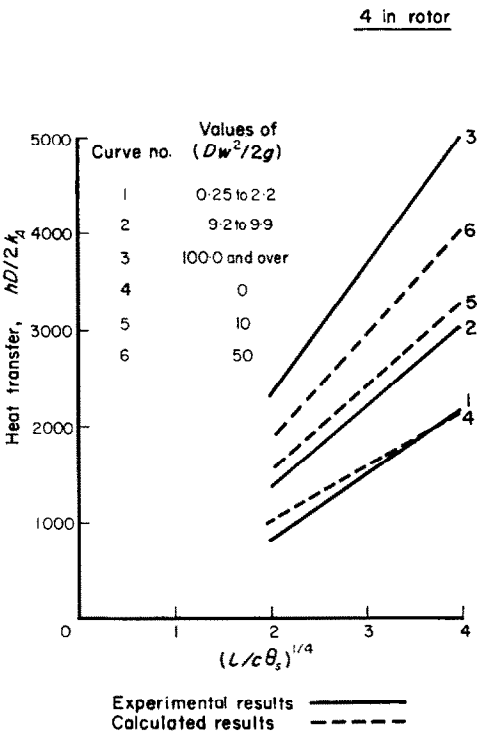

FIG. 10. Comparison of calculated with experimental results for the 4 in rotor.

drops. At the instant of parting from the water layer the equilibrium of a hemispherical drop depends on its radial acceleration force

$$\left(\frac{\rho}{g} \cdot \frac{2\pi d^3}{3\ 8}, \cdot \frac{D\,w^2}{4}\right)$$

and also on the surface-tension force ($\pi d\sigma$) where d is the diameter of drop. At the moment of throwing off, these two forces are equal and $(\rho d^2 . D\,w^2/2g) = (12\sigma)$ or, for any value of $(D\,w^2/2g)$,

$$d \propto \sqrt{(\sigma/\rho)}$$

The ratio D/d of cylinder diameter to drop diameter is thus proportional to the non-dimensional function $D\sqrt{(\rho/\sigma)}$, and statistical analysis of the experimental results has given, as an optimum expression for B_1,

$$B_1 = 1{\cdot}5\,[D\sqrt{(\rho/\sigma)}]^{-0{\cdot}19}\,(1{\cdot}9 - 0{\cdot}9/1{\cdot}095^{D\,w^2/2g}) \quad (9)$$

4.5 *Variation of heat transfer with the nature of the rotor's surface*

The nature of the surface of the rotor is the fifth independent variable referred to in Section 4.1. This has been kept as nearly as possible constant throughout the tests by,

(*a*) plating the surface with a 0·001 in thick layer of nickel as mentioned in Section 2.2,
(*b*) by cleaning the surface in the manner described in Section 2.3.

4.6 *A recommended equation*

The ranges of independent variables considered were

(*a*) steam temperatures T_s of 220° to 310°F;
(*b*) differences θ_s between steam and rotor temperatures of 6 to 50 degF;
(*c*) speeds of rotation of 0 to 1500 rev/min;
(*d*) rotor diameters D of 4, 8, and 10 in.

It appears that inside these ranges a formula for the heat-transfer coefficient can be expressed, after substituting in equation (6) the value for B_1 given by equations (8) and (9), as follows:

$$h = 1{\cdot}5\,[D\sqrt{(\rho/\sigma)}]^{-0{\cdot}19}\,(1{\cdot}9 - 0{\cdot}9/1{\cdot}095^{D\,w^2/2g})\,(k^3\,g\,\rho^2\,c/D\,\mu)^{1/4}\,(l/c\,\theta_s)^{1/4} \quad (10)$$

or, in non-dimensional terms,

$$hD/2\,k_A = 0{\cdot}75\,[D\sqrt{(\rho/\sigma)}]^{-0{\cdot}19}\,(1{\cdot}9 - 0{\cdot}9/1{\cdot}095^{D\,w^2/2g})\,(k^3\,g\,\rho^2\,c\,D^3/\mu\,k_A^4)^{1/4}\,(l/c\,\theta_s)^{1/4} \quad (11)$$

If values of $(hD/2\,k_A)$, taken from equation (11) and based on various values of θ_s, are plotted against $(l/c\,\theta_s)^{1/4}$ at values of $D\,w^2/2g$ of 0, 20, and 50, using steam and condensate properties at an arbitrarily selected temperature of 235°F, the broken lines in Figs. 8, 9, and 10 are obtained showing a comparison between the calculated and experimentally found coefficients.

If the heat-transfer coefficients are calculated for each of nearly 180 test results separately, using equation (10), and if the values of h so calculated are compared with the experimental values of h found from equation (2) the following correlation appears. In the case of the 4, 8, and 10 in rotors respectively the arithmetic means of the experimental results are 2260, 2230, and 1720 Btu/ft²h degF. The roots of the mean squares of the deviations of the calculated from the experimental results are 351, 287, and 240 Btu/ft²h degF, or 15·5, 12·9, and 16·8 per cent of the mean calculated coefficients. The ranges of variables studied cover the most severe part of the starting conditions in many modern turbines and the recommended equation is therefore of considerable use in investigations of conditions in turbines while starting from cold.

4.7. *Comparison with results of other workers*

Yeh [2] and Singer and Preckshot [7], carried out similar work on 1 in dia. rotors. Expressed in terms of the variation of $hD/2\,k_A$ with the Weber number $(D\sqrt{(\rho/\sigma)})^2(D\,w^2/2g)/2$, some of

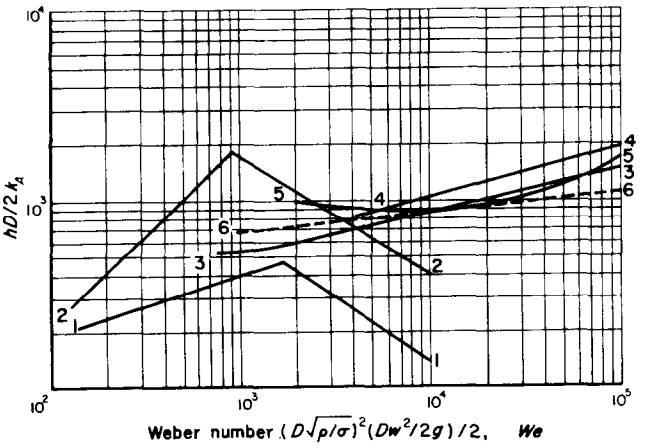

FIG. 11. Comparison of results obtained by the authors with results obtained by other workers in the same field.

Yeh's results are given by the curve 1–1 in Fig. 11 and Singer and Preckshot's are given by curve 2–2. The authors' results for the 4, 8 and 10 in dia. rotors respectively are given by curves 3–3, 4–4 and 5–5. Values for the 4 in rotor calculated using equation (11) are shown by the line 6–6 for comparison with the experimental line 3–3.

The most noticeable feature of the comparison between the authors' and others' work is the absence in the authors' of the decline of the heat-transfer coefficient at values of the Weber number above 1700 in Yeh's and 900 in Singer and Preckshot's case. Why the decline was observed by them and not by the authors is not known but the investigation is now continuing with the objects (*a*) of studying in one apparatus the range of varying diameters from 1 in upwards, and also (*b*) of modifying equation 10 to make it relevant to ranges of variables outside those investigated here.

ACKNOWLEDGEMENTS

The work reported here was carried out on behalf of the Director General Ships, Admiralty, to whom our thanks are due for permission to publish.

REFERENCES

1. N. NUSSELT, Die Oberflachenkondensation des Wasserdampfes, *Z. Ver. Deut. Ing.* **60**, 541 (1916).
2. L. YEH, The effect of surface speed and steam pressures upon the transfer of heat from steam to a rotating cylinder, Ph.D. thesis, London (1954).
3. C. M. COOPER, T. B. DREW and W. H. MCADAMS, The isothermal flow of liquid layers, *Ind. & Engng Chem.* **26**, 428 (1934).
4. R. HOYLE and D. H. MATTHEWS, The condition of the condensate layer on a cold cylinder rotating in a steam atmosphere (to be published).
5. C. C. MONRAD and W. L. BADGER, The condensation of vapours, *Ind. & Engng Chem.* **22**, 1103 (1930).
6. E. M. SPARROW and J. L. GREGG, Trans. *Amer. Soc. Mech. Engrs*, Series C, *J. Heat Transfer*, (a) A theory of rotating condensation, **81**, 113 (1959); (b) The effect of vapour drag on rotating condensation, **82**, 71 (1960); (c) A boundary-layer treatment of laminar-film condensation, **81**, 13 (1959); (d) Laminar condensation heat transfer on a horizontal cylinder, **81**, 291 (1959).
7. R. M. SINGER and G. W. PRECKSHOT, The condensation of vapour on a horizontal rotating cylinder, *Proc. Heat Transfer and Fluid Mechanics Inst.* No. 14, p. 205 (1963).
8. R. W. POWELL, Experiments using a simple thermal comparator for measurement of thermal conductivity, surface roughness, and thickness of foils or surface deposits, *J. Sci. Instrum.* **34**, 485 (1957).

Résumé—On décrit un appareil pour mesurer le transport de chaleur à partir d'une atmosphère de vapeur d'eau à des cylindres tournants refroidis sur lesquels la vapeur se condense. Trois cylindres de 10, 20 et 25 cm de diamètre chacun refroidis à l'intérieur par de l'eau ont été utilisés. La grandeur du flux de chaleur à partir de l'atmosphère de vapeur d'eau a été calculée à partir de mesures des gradients de températures à travers les parois du rotor. On a fait une comparaison, dans le cas stationnaire, entre les résultats mesurés et ceux calculés à partir de l'équation de Nusselt. Pour le cas en rotation, l'équation de Nusselt a été modifiée, et on a montré comment cette équation modifiée peut être employée dans le calcul des coefficients de transport de chaleur pour n'importe quelle température, diamètre et vitesse de rotation dans les gammes considérées. Les gammes de vitesses allaient de 0 à 1500 tours par minute, celles de température de condensation allaient de 104°C à 154°C, et celles de différence de température entre le vapeur et le rotor allaient de 3,3°C et 27,8°C. Ces gammes couvrent les conditions existant dans beaucoup de turbines à vapeur pendant le départ à froid et dans quelques condenseurs tournants.

Zusammenfussung—Es wird eine Versuchsanordnung beschrieben zur Messung des Wärmeüberganges auf gekühlte, rotierende Zylinder in einer kondensierenden Dampfatmosphäre, Drei Zylinder von 10,16, 20,32 und 25,4 cm Durchmesser, die inwendig mit Wasser gekühlt werden können, wurden verwendet. Die Grösse des Wärmestroms aus der Dampfatmosphäre wurde durch Messungen der Temperaturgradienten in den Rotorwänden ermittelt. Für den stationären Fall wurden die Messergebnisse mit berechneten Werten der Nusselt-Gleichung verglichen. Für den zylindrischen Fall ist die Nusselt-Zahl modifiziert worden und es wird gezeigt, wie diese modifizierte Gleichung für Wärmeübergangsberechnungen bei beliebigen Temperaturen, Durchmesser und Rotationsgeschwindigkeiten im betrachteten Bereich verwendet werden kann. Der Geschwindigkeitsbereich reicht von 0 bis 1500 Umdrehungen/min, der der Kondensationstemperaturen von 104,5°C ,bis 154,5°C und der der Temperaturdifferenzen zwischen Dampf und Rotor von 3,3 bis 27,8 grdC. Diese Bereiche stimmen mit Bedingungen überein, wie sie für Dampfturbinen vorliegen, die im kalten Zustand angefahren werden, sowie in etwa für rotierende Kondensatoren.

Аннотация—Описан прибор для измерения теплообмена между охлаждаемыми вращающимися цилиндрами и атмосферой водяного пара, который конденсируется на их поверхности.

Величина теплового потока из атмосферы водяного пара вычислялась на основании измерений температурных градиентов в стенках ротора. Результаты измерений сравнивались с величинами, подсчитанными по уравнению Нуссельта в стационарном состоянии. Показано, как модифицированное для условий вращения уравнение Нуссельта может быть использовано при вычислении коэффициентов теплообмена для любой температуры, диаметра и скорости вращения в пределах рассматриваемых величин. Исследовались скорости от 0 до 1500 об/мин, температуры конденсации пара от 220°F до 310°F, температурные разности пара и потери от 6 до 50°F. Такие диапазоны параметров встречаются во многих паровых турбинах в период пуска, а также в некоторых вращающихся конденсаторах.